Estimation of mechanical properties of panels based on modal density and mean mobility measurements

Benjamin Elie[1,*], François Gautier

LAUM, UMR CNRS 6613, Avenue Olivier Messiaen F-72085 Le Mans Cedex 9

Bertrand David

Institut Mines-Télécom, Télécom ParisTech, CNRS LTCI 46 rue Barrault F-75634 Paris Cedex 13

Abstract

The mechanical characteristics of wood panels used by instrument makers are related to numerous factors, including the nature of the wood or characteristic of the wood sample (direction of fibers, micro-structure nature). This leads to variations in the Young's modulus, the mass density, and the damping coefficients. Existing methods for estimating these parameters are not suitable for instrument makers, mainly because of the need of expensive experimental setups, or complicated protocols, which are not adapted to a daily practice in a workshop. In this paper, a method for estimating the Young's modulus, the mass density, and the modal loss factors of flat panels, requiring a few measurement points and an affordable experimental setup, is presented. It is based on the estimation of two characteristic quantities: the modal density and the mean mobility. The modal density is computed from the values of the modal frequencies estimated by the subspace method

*Corresponding author. Tel: +33 243833289

Email address: benjamin.elie.etu@univ-lemans.fr (Benjamin Elie)

ESPRIT (*Estimation of Signal Parameters via Rotational Invariance Techniques*), associated with the signal enumeration technique ESTER (*ESTimation of ERror*). This modal identification technique is proved to be robust in the low- and the mid-frequency domains, *i.e.* when the modal overlap factor does not exceed 1. The estimation of the modal parameters also enables the computation of the modal loss factor in the low- and the mid-frequency domains. An experimental fit with the theoretical expressions for the modal density and the mean mobility enables an accurate estimation of the Young's modulus and the mass density of flat panels. A numerical and an experimental study show that the method is robust, and that it requires solely a few measurement points.
Keywords:
Mode density, Modal identification, Subspace method, Mid-frequency, Wood, Stringed instrument making

1. Introduction

This study stems from a musical acoustics problematic related to the characterization of materials used for the manufacturing of string instrument soundboards. The choice of the material is an essential part of the luthier's savoir-faire, and the characterization of woods used to make string instruments has been investigated [1, 2].

The mechanical characteristics of wood panels used by instrument makers are related to numerous factors, including the nature of the wood or characteristic of the wood sample (direction of fibers, micro-structure nature). This leads to different values of the Young's modulus, the mass density, and

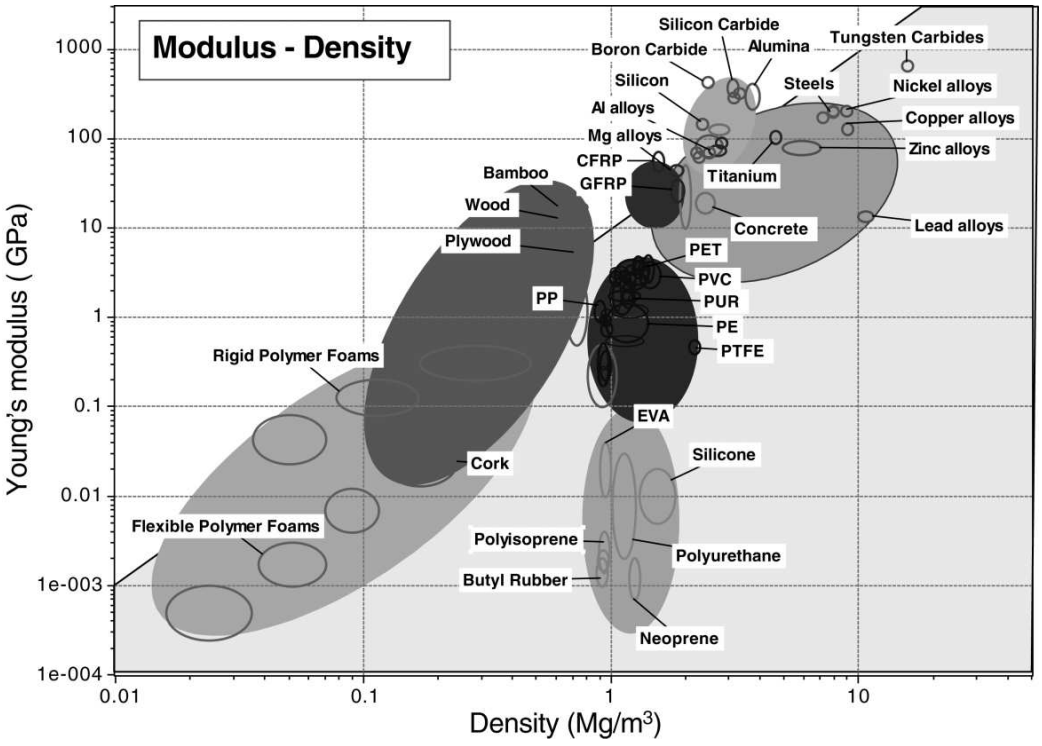

Figure 1: Classification of materials using the Young's modulus - mass density plane (from Ashby *et al.* [3]).

the damping coefficients, according to the choice of the used sample. These intrinsic parameters are commonly used to discriminate materials and enable their clustering. The most noticeable example is the Ashby diagram [3], displayed in Figure 1.

The knowledge of these parameters is important for the luthier to make its choice. Several methods exist for accurately estimating the mechanical properties of materials. Their domain of relevance is defined by the order of magnitude of the Young's modulus of the material and the frequency bounds [4]. Among them, the DMA (*Dynamic Mechanical Analysis*) [5]

is relevant in the low-frequency domain. Another technique is the Oberst beam method [6], which is based on a modal fit of the first resonances of a clamped beam. It has been widely used and studied [7, 8]. In the high-frequency domain, ultrasonic methods [9] are more commonly applied on both liquid [10] or solid materials [11]. Yet, these methods usually require either expensive laboratory devices or complicated protocols. Thus, they are not suitable for a daily practice in a luthier's workshop.

We propose a method based on the analysis of the mechanical frequency response function, measured on flat panels. Such a method is designed to perform a non-restrictive practice *in situ*. The estimation of quantities, namely the modal density and the mean mobility, enables an estimation of the bending stiffness and the mass density of the tested panel. These intrinsic parameters can be obtained via this method, using solely a few transfer function measurements.

In Section 2, the whole method for estimating *in fine* the bending stiffness, the mass density, and the modal loss factor is presented. The performance of the method under several constraints (large modal overlap, weak signal-to-noise ratio, excitation on a nodal line) is studied in Section 3, by means of numerical simulations. Finally, Section 4 presents experimental applications of the method on metallic and wood panels.

2. Method for estimating the Young's modulus, the mass density, and the modal loss factor of a flat panel

2.1. Principle of the method

The input mobility of a structure is the ratio in the frequency domain between the velocity of the structure $V(\omega)$ and the excitation force $F(\omega)$, and can be easily measured using standard modal testing devices. From this measurement, it is possible to identify the modal parameters associated to the structure. These quantities (input admittance and modal parameters) basically depend on the geometry of the panel, and on its mechanical properties, namely the Young's modulus E and the mass density ρ.

In this section, we present first the modal description of the input mobility of a panel and the modal identification technique used for the study. Then, the method for estimating the Young's modulus, the mass density, and the modal loss factor is presented. It is based on an experimental estimation of the modal density and the mean mobility of the panel. Then, the knowledge of these quantities enables to estimate the values of E and ρ minimizing the differences between theoretical models of mean mobility and modal density of panels. The modal loss factor is directly derived from the estimated modal parameters, using a modal identification technique described in Section 2.3.

2.2. Modal description of the input mobility of a flat panel

The method presented in this paper is based on driving-point mechanical admittance (or mobility) measurements. It is commonly denoted $Y(\omega)$, and can be developed on the basis of the complex modes as [12]:

$$Y_A(\omega) = j\omega \sum_{k=1}^{N} \left\{ \frac{u_k^2(A)}{\alpha_k + j(\omega + \omega_k)} + \frac{\bar{u}_k^2(A)}{\alpha_k + j(\omega - \omega_k)} \right\}, \tag{1}$$

$$u_k^2(A) = \frac{\Phi_k^2(A)}{2j\omega_k m_k}, \tag{2}$$

where A denotes the driving-point, ω_k, α_k, m_k and Φ_k are respectively the modal angular frequency, the modal damping factor, the modal mass and the modal shape associated to the k^{th} mode. $\bar{u}_k$ denotes the complex conjugate of u_k, the complex modal amplitude of the k^{th} mode. The number of eigenmodes in the frequency band of analysis is denoted by the symbol N.

If the damping matrix is such that the mode shapes Φ_k are real, which is the case if the Caughey condition is satisfied [13], then Eq. (2) can be rewritten in the form:

$$Y_A(\omega) = j\omega \sum_{k=1}^{N} \frac{\Phi_k^2(A)}{m_k(\omega_k^2 + j\eta_k\omega_k\omega - \omega^2)}, \tag{3}$$

where $\eta_k = \frac{\alpha_k}{\pi f_k}$ denotes the modal loss factor of k^{th} mode.

A straightforward method to estimate the driving-point mobility is to record the acceleration signal, via a small accelerometer, of the structure, when it is submitted to an impulse force, performed by a small impact hammer at the driving-point location. Figure 2 shows the mechanical admittance of a $500 \times 190 \times 2$ mm spruce flat panel used for guitar soundboard manufacturing. The panel is hanged with wires to create free edges conditions. The acceleration and force signals are obtained at the same location, using a small accelerometer PCB Piezotronics 352C23 (0.2 g) and a small impact hammer PCB Piezotronics 086E80.

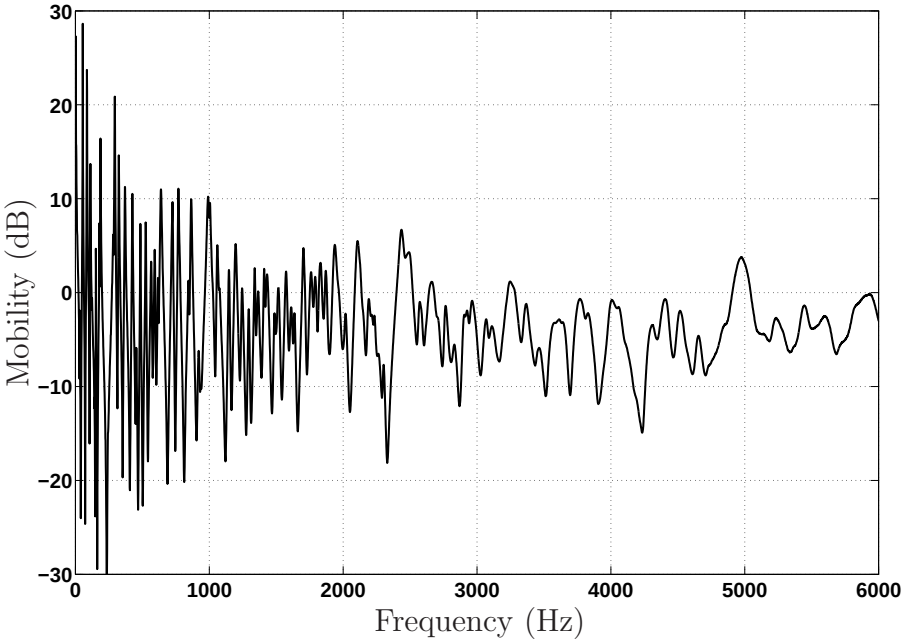

Figure 2: Driving-point mobility of the $500 \times 190 \times 2$ mm spruce panel. The reference at 0 dB corresponds to a mobility of 0.094 m.s^{-1}/N, namely the mobility of a 2mm-thick finite panel having the typical mechanical properties of spruce.

Figure 2 highlights the superimposition of modal contributions expressed in Eq. (3). The visible peaks in the mechanical admittance are associated to modal contributions. Their overlap increases with the frequency.

2.3. Modal identification techniques

Many techniques have been developed for estimating modal parameters from measured transfer functions. Reviews of existing methodologies for experimental modal analysis are available in Refs [14, 15]. It is known that these methods are no longer robust when the modal overlap increases in the mid- and the high-frequency domains [16, 17]. Subspace methods like MUSIC (*MUltiple SIgnal Classification*) [18], Matrix Pencil [19], or ESPRIT (*Estimation of Signal Parameters via Rotational Invariance Techniques*) [20] are then interesting to consider and have already been successfully applied to vibration signals [21–27]. Indeed, these methods overcome the Fourier resolution limit and are then useful when modes are overlapping, hence the designation *high-resolution*. In this work, ESPRIT is used since it is known to be one of the more robust.

2.3.1. ESPRIT algorithm

The velocity response $s(A,t)$ to an impulse force is the real part of the inverse Fourier transform of the driving-point mobility $Y_A(\omega)$. It is the real part of the sum of complex damped sinusoids, each one being the time response of a mode:

$$s(A,t) = \Re\left[\sum_{k=1}^{K} b_k(A) z_k^t\right], \tag{4}$$

where $b_k(A) = a_k(A)e^{j\varphi_k(A)}$ is the complex amplitude of the k-th mode, and $z_k = e^{-\alpha_k + j\omega_k}$ denotes the corresponding pole with modal pulsation ω_k and damping factor α_k. K is the number of complex poles in the frequency band $[-F_s/2 \quad F_s/2]$, where F_s is the sampling frequency ($K = 2N$).

The ESPRIT [20] algorithm estimates the signal parameters corresponding to the modal parameters of the K sinusoidal components embedded in the signal. As the other subspace high resolution methods (such as Matrix Pencil or MUSIC), it is based on the decomposition of the data vector space onto two orthogonal subspaces, the so-called signal and noise subspaces. Then, using the so-called rotational invariance property of the signal subspace (it remains invariant from a sample to the next), the poles z_k spanning the signal subspace can be estimated accurately. The reader can refer to Ref. [26] for a detailed description of the ESPRIT algorithm. The subspace decomposition and the use of the rotational invariance property make the ESPRIT method more robust and accurate than classic Prony-based method, such as LSCE [14] for instance.

2.3.2. Signal enumeration technique

An important issue when applying subspace methods to composite signals is the tuning of the modeling order K, which is usually unknown. Several methods have been proposed to estimate K: the maximum likelihood [28] method and Information Theoretic Criteria (ITC) [29], which include the Akaike Information Criteria (AIC) [30], and the Maximum Description Length (MDL) [31]. More recently, the ESTER (*ESTimation of ERror*) criterion, based on the assessment of the rotational invariance property that characterizes the signal subspace, has been designed by Badeau *et*

al. [23] and used by Ege [24] and Elie *et al.* [26] in the context of musical acoustics. We thus chose to apply this technique since it proves reliable and also for its straightforward implementation with the ESPRIT algorithm.

This criterion consists in appraising the rotational invariance property of the signal sub-space with an error function. This latter being minimal when the rotational invariance property is verified, namely when the modeling order is equal to the right number of sinusoidal components. Note that for impulse responses signal, which is real, the number of components K is twice the number of physical eigenmodes.

The identified modes using ESPRIT and ESTER techniques enable us to compute the modal density of the panel. Theoretical and practical estimation of the modal density are given in Section 2.4.

2.4. Modal density of flat panels

The method developed by Courant [32] to compute the modal density of a rectangular plate is based on the estimation of the mode count function, denoted $N(\Omega)$, which is the number of modes having an angular frequency less than the angular frequency Ω. The modal density $n(\Omega)$ is then the derivative of $N(\Omega)$ with respect to Ω.

2.4.1. Asymptotic value of the modal density

Courant [32], then Wilkinson [33], give the expressions of the asymptotic value of the modal density of a rectangular panel, in the isotropic and the orthotropic case, when the frequency tends to an infinite value. After [32] and [33], it is shown that

$$n(\omega) \underset{\omega\to\infty}{\to} \alpha \frac{S}{4\pi}\sqrt{\frac{\rho h}{D^*}}, \tag{5}$$

with

$$\begin{cases} \alpha = 1 \\ D^* = \frac{Eh^3}{12(1-\nu^2)}, \end{cases} \tag{6}$$

for an isotropic material, and

$$\begin{cases} \alpha = \frac{2}{\pi}F(\frac{\pi}{2},\chi) \\ D^* = \frac{\pi^2}{4}\frac{\sqrt{D_1 D_3}}{F^2\left(\frac{\pi}{2},\chi\right)}, \end{cases} \tag{7}$$

for an orthotropic material.

In Eq. (5), S is the surface of the plate, h and ρ are respectively the thickness and the mass density of the plate, D^* is its bending stiffness modulus. For an orthotropic material, the equivalent bending stiffness depends on 4 constants $D_{i=1,\cdots,4}$ accounting for the orthotropic nature of the material. In Eq. (6) and (7), E is the Young's modulus, ν is the Poisson ratio. $F(\frac{\pi}{2},\chi) = \int_0^{\frac{\pi}{2}} \left[1-\chi^2\sin^2(2\theta)\right]^{-\frac{1}{2}} d\theta$ is the complete elliptic integral of the first kind, where $\chi = \sqrt{\frac{1}{2}\left(1-\frac{D_2+D_4}{2\sqrt{D_1 D_3}}\right)}$.

Eq. (5) suggests that it is possible to express the modal density of any orthotropic plate as the modal density of an equivalent isotropic plate, having the equivalent bending stiffness D^*. The associated equivalent Young's modulus is then

$$E^* = \sqrt{E_x E_y}. \tag{8}$$

2.4.2. Effects of the boundary conditions

Xie *et al.* [34] give corrections of the asymptotic modal density taking the boundary conditions into accounts. The modal density of a rectangular flat panel writes

$$n(\omega) = n_\infty + n_c \omega^{-1/2}, \tag{9}$$

where n_∞ is the asymptotic value of the plate, from Eq. (5). The term n_c is an additive term depending on the boundary conditions:

1. $n_c = -\frac{L_x+L_y}{2}\sqrt{\frac{\rho h}{D}}$ for a simply-supported panel.
2. $n_c = (L_x + L_y)\sqrt{\frac{\rho h}{D}}$ for a free-edges panel.

In the low-frequency domain, the corrections are important. However, they tend to be negligible in the mid- and the high-frequency domains.

Note that the modal density can be written as

$$n(\omega) = p\beta + q\sqrt{\beta/f}, \tag{10}$$

where $p = \frac{S}{4\pi}$, q is a constant coefficient depending on the boundary conditions and on the perimeter of the plate, and $\beta = \sqrt{\frac{\rho h}{D}}$ is called the *plate elastic constant*, depending on the mechanical properties of the material.

2.4.3. Estimation of the analytical modal density from the discrete modal frequencies

In practice, the modal density can be estimated from the values of the modal frequencies. The discrete modal density n_k is then the inverse of the frequency distance between two successive modes:

$$n_k = \frac{1}{f_{k+1} - f_k}. \tag{11}$$

Figure 3 shows an example of the discrete and analytical modal density computed for two simulated plates. One with an isotropic material, and the other one with an orthotropic material.

Figure 3 shows that the discrete modal density is a good approximation of the analytical modal density. The model of the modal density in Eq. (5) can thus be used to fit experimental data.

In practice, the estimation of the plate elastic constant can be performed by minimizing the differences between the estimated modal density and the analytical modal density model in the least square sense:

$$\beta = \underset{\hat{\beta}}{\operatorname{argmin}} \left|\left| \mathbf{n} - p\hat{\beta} + q\sqrt{\hat{\beta}}\mathbf{g} \right|\right|_2^2, \tag{12}$$

where $\mathbf{n} \in \mathbb{R}_+^{*N}$ is a vector containing the N measured values of the modal density, *i.e.* $\mathbf{n} = [n_1 \quad n_2 \quad \cdots \quad n_{\tilde{K}}]$, $\tilde{K}$ being the number of modes estimated in the impulse response. The vector $\mathbf{g} \in \mathbb{R}_+^{*N}$ is the vector containing the N square roots of the inverse measured modal frequencies, *i.e.* $\mathbf{g} = [f_1^{-1/2} \quad f_2^{-1/2} \quad \cdots \quad f_{\tilde{K}}^{-1/2}]$.

The estimation of β, using Eq. (12), provides a first relationship between the Young's modulus E and the mass density ρ. A second one is needed and is given by the analysis of the mean-value of mobility, performed in Section 2.5.

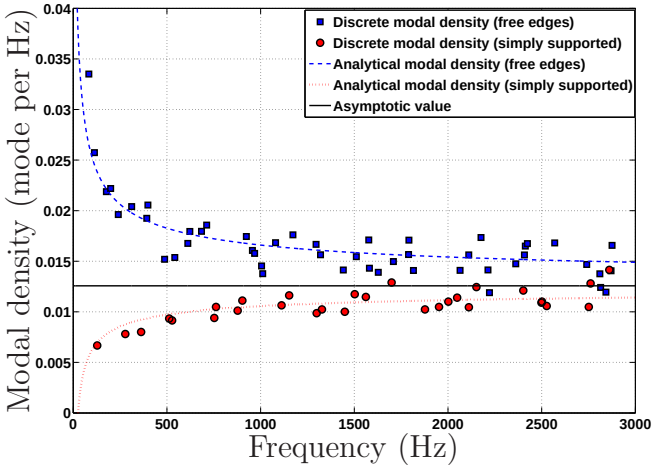

(a)

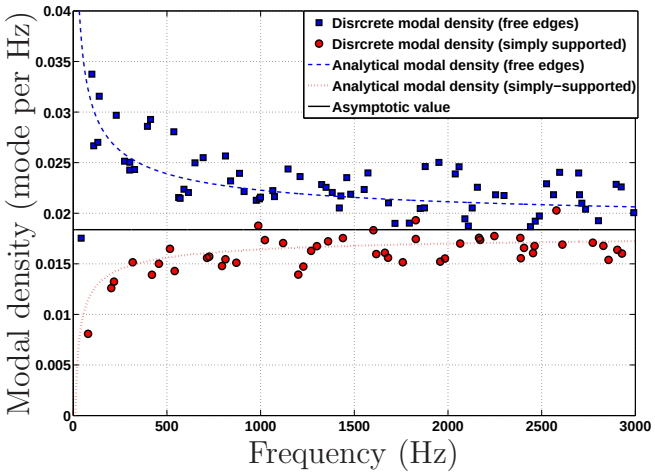

(b)

Figure 3: a) Example of modal density of an aluminum plate ($L_x = 0.28$ m, $L_y = 0.35$ m, $h = 2.5$ mm, $\rho = 2700\ kg.m^{-3}$, $E = 70$ GPa) b) Example of modal density of a maple plate ($L_x = 0.32$ m, $L_y = 0.20$ m, $h = 2.5$ mm, $\rho = 650\ kg.m^{-3}$, $D_{i=1,..,4} = [13.4, 2.19, 2.66, 3.59]$ N.m).

2.5. Mean-value of mobility

2.5.1. Definition

The so-called mean-value, or characteristic admittance Y_C, of a finite structure is defined by Skudrzyk [35] as the mobility of the equivalent structure with infinite dimensions. Skudrzyk [35] derives a closed-form expression to estimate the real part of the characteristic admittance, $G_C = \Re\left(Y_C\right)$, of the finite structure from its properties:

$$G_C(\omega) = \frac{\pi n(\omega)}{2M_{Tot}}, \tag{13}$$

where $n(\omega)$ denotes the local modal density of the finite structure and M_{Tot} is the total mass of the system.

Equation (13) is based upon several assumptions:

1. the modal overlap is supposed to be large enough, so that the modal contributions are no longer individually observable,
2. the structure is supposed to be homogeneous (the surface density is constant over the whole structure),
3. the generalized damping matrix is supposed to be diagonal (Basile hypothesis),
4. the modal loss factor is assumed to be constant over the whole frequency range.

The above hypotheses are in particular valid for plate-like systems, for which analytical expressions of modal density have been previously proposed [32–34, 36].

The substitution of Equation (5) in (13) leads to the expression of the asymptotic value of the characteristic admittance of rectangular flat panels:

$$G_{C_\infty} = \frac{1}{8\sqrt{\rho h D}}. \tag{14}$$

The value of G_{C_∞} can be used as an indicator to quantify the ability of the structure to vibrate, a structure with large characteristic admittance being globally more mobile, therefore more efficient to vibrate.

In the case of conservative thin plates, the imaginary part of the mobility of an infinite plate is zero (*cf.* Ref. [16], pages 34-39), therefore the imaginary part of the characteristic admittance is null.

2.5.2. Estimation of the mean-value of mobility G_C

To estimate the mean-value of mobility as defined by Skudrzyk [35], we use one of its properties: it is the mobility of the structure if all modes were non-resonant. This configuration can be reached by multiplying the velocity response by an exponential window $e^{-\alpha_w t}$, where α_w is a damping parameter. This kind of windowing for the velocity response induces an additional damping to each mode. The velocity response writes

$$s(t) = \sum_{k=1}^{N} b_k e^{2j\pi f_k t - \alpha_k t} e^{-\alpha_w t} = \sum_{k=1}^{N} b_k e^{2j\pi f_k t - (\alpha_k + \alpha_w) t}, \tag{15}$$

where b_k, α_k, and f_k are respectively the complex amplitude, the damping coefficient, and the frequency of the mode k. An example of mobilities of the same structure with different α_w is displayed in Figure 4.

2.6. Estimation of M, D^*, and the modal loss factor

The estimation of the mass density ρ uses Equation (13). The estimated mass is the mass M such that the ratio $\frac{n_{fit}}{4M}$, where n_{fit} is the estimated

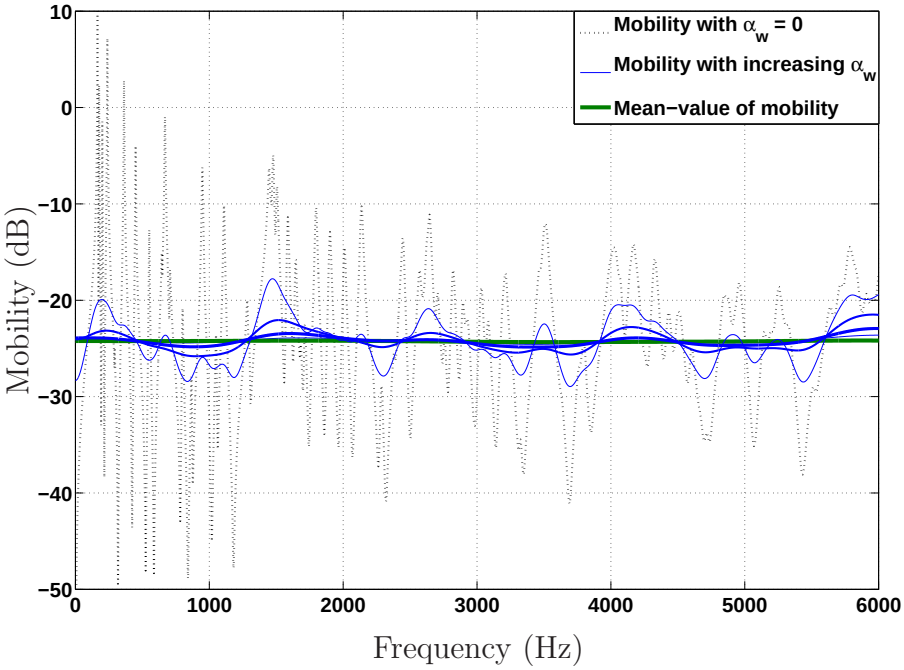

Figure 4: Mobility of a simulated plate with different values of the damping parameter α_w. When α_w is large enough, the mobility is then a straight line, corresponding to the mean-value of mobility.

analytical modal density, minimizes in a least square sense the differences with the mean-value of mobility G_C, hence

$$M = \underset{\hat{M}}{\operatorname{argmin}} \| G_C - \frac{n}{4\hat{M}} \|_2^2. \tag{16}$$

The value α_w used to compute G_C should be set to a very large value. In practice, the mass M is estimated several times for increasing values of α_w. The process stops when the ration between the estimated mass M_k at the iteration k and M_{k-1} is under an arbitrary threshold ϵ, set to 0.01%.

The mass density is then

$$\rho = \frac{M}{V}, \tag{17}$$

where V is the volume of the plate. Finally, the bending stiffness D^* is given by

$$D^* = \frac{\rho h}{\beta^2}. \tag{18}$$

The modal loss factor η_k is computed directly from the values of the modal damping coefficients α_k and the modal angular frequencies ω_k estimated by ESPRIT:

$$\eta_k = \frac{2\alpha_k}{\omega_k}. \tag{19}$$

The procedure for estimating the mass density ρ and the Young's modulus E can be summarized as follows:

1. the elastic plate constant is estimated from Eq. (12), using the modal density estimated by the combination of the ESPRIT and ESTER techniques,

2. the mass of the system is found from Eq. (16), using an estimation of the mean mobility G_C,
3. the values of ρ and E are deduced from M and β, using Eq. (18) and (6),
4. the modal loss factor is computed from the modal parameters estimated by ESPRIT using Eq. (19).

It is worth noting that our method does not require a more specialized equipment like laser interferometers or traction measurement systems and is thus useful to be employed in a luthier workshop context.

3. Validation of the method

3.1. Limits of the enumeration technique

The methodology is based on an accurate estimation of the modal density. The aim of this section is to study the limitation of the enumeration technique when it is subjected to different conditions likely to fault the method. For that purpose, tests on *hybrid* impulse responses are subjected to the enumeration procedure. The interest is to accurately simulate the experimental conditions. The method accuracy depends on the following factors:

1. the modal density of the structure,
2. the damping factor of the sinusoidal components,
3. the signal-to-noise ratio,
4. the position of the observation and excitation point. Indeed, applying the method in an unique point may induce a bias, if the excitation or observation point is on a nodal line, for instance. A node excitation is likely to make them barely detectable.

The simulated signals are designed by mixing a thin plate modal superimposition and measured noise outcomes obtained from typical vibro-acoustic sensor; hence the denomination "Hybrid". The reader may refer to Ref. [26] for a detailed description of the hybrid synthesis of impulse responses.

3.1.1. Results

We propose to investigate the limits of the method related to too high values of the modal density n, the modal loss factor η, and the noise level, as well as the driving-point position. We chose a nominal configuration for a simulated plate as the starting point of different parametric tests. The modal overlap factor is defined as $\mu = \eta n f$, where n is the asymptotic value of the modal density, and η is the modal loss factor.

The first test consists in simulating impulse responses of plates with different values of n et η. Then it consists in varying the signal-to-noise ratio. The last test focuses on the sensibility of the method accuracy to the observation and excitation point. For each parameter, we define a nominal value. During the test procedures, solely one parameter varies, the other parameters are set to their nominal value. Table 1 gives the chosen nominal values for the test.

Influence of the modal density and damping

The considered value of the modal density n is the asymptotic value n_∞ given by Eq. (5). The modal density is modified by changing the area S, the other parameters (stiffness, mass density, thickness and damping) are kept constant, set to their nominal value (*cf.* Table 1) along the procedure. Then, a similar test, consisting in varying solely the modal loss factor, is performed.

Table 1: Chosen nominal values for every parameter used in the hybrid impulse responses syntheses.

Parameter	Unit	Value
Plate length	m	0.5
Plate width	m	0.19
Plate thickness	m	2.5×10^{-3}
Volumic mass	kg.m^{-3}	420
Loss factor	%	1
D_1	N.m	17.2
D_2	N.m	1.05
D_3	N.m	1.31
D_4	N.m	1.87
Maximum frequency of analysis	Hz	2700

The results of both tests are displayed in Figure 5. It represents the error ratio $\Delta K/K = \frac{K_est-K}{K}$, where K_{est} is the estimated number of components and K is the right number of components.

The test confirms the accuracy of the method to estimate the right number of modes, even when the modal overlap is large. However, this accuracy tends to deteriorate when the modal overlap factor exceeds 100 %. The method is therefore robust in the low- and in the mid- frequency ranges.

Influence of the signal-to-noise ratio

The influence of the signal-to-noise ratio on the method robustness is tested according to the following procedure: every mechanical and geometrical parameters of the simulated plates are set to their nominal value, the

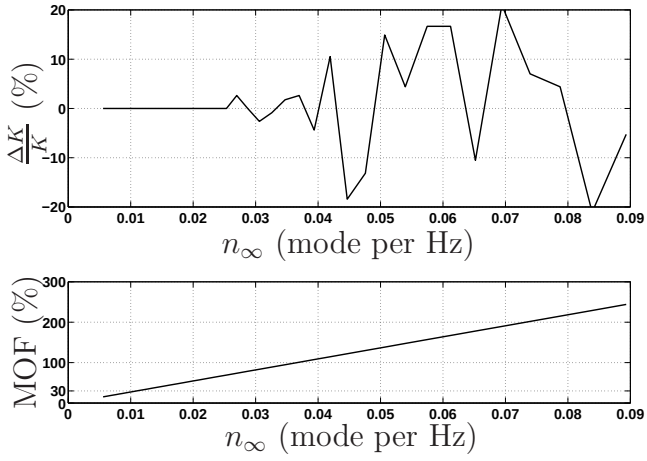

(a)

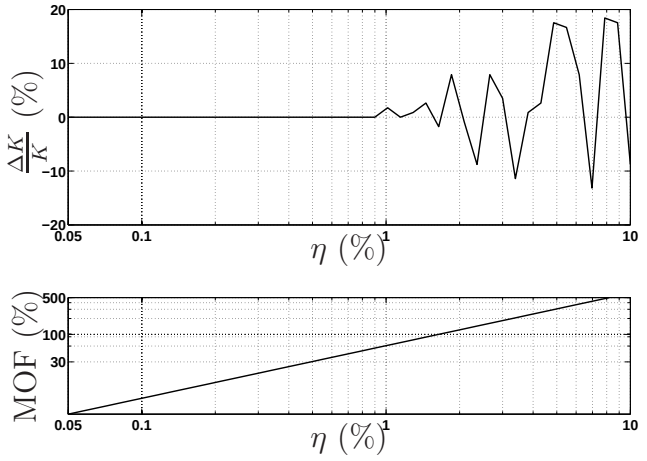

(b)

Figure 5: Enumeration accuracy as a function of a) the modal density, and b) the modal loss factor

signal-to-noise ratio is modified by controlling the excitation level, *i.e.* the level of the simulated force signal. The signal-to-noise ratio is then defined

by the following relation:

$$RSB = 20 \log_{10} \left[\frac{A_\gamma}{A_{n_\gamma}} \right], \tag{20}$$

where A_γ is the RMS (*Root Mean Square*) value of the noiseless simulated acceleration signal, and A_{n_γ} is the RMS value of the noise signal, recorded on the accelerometer.

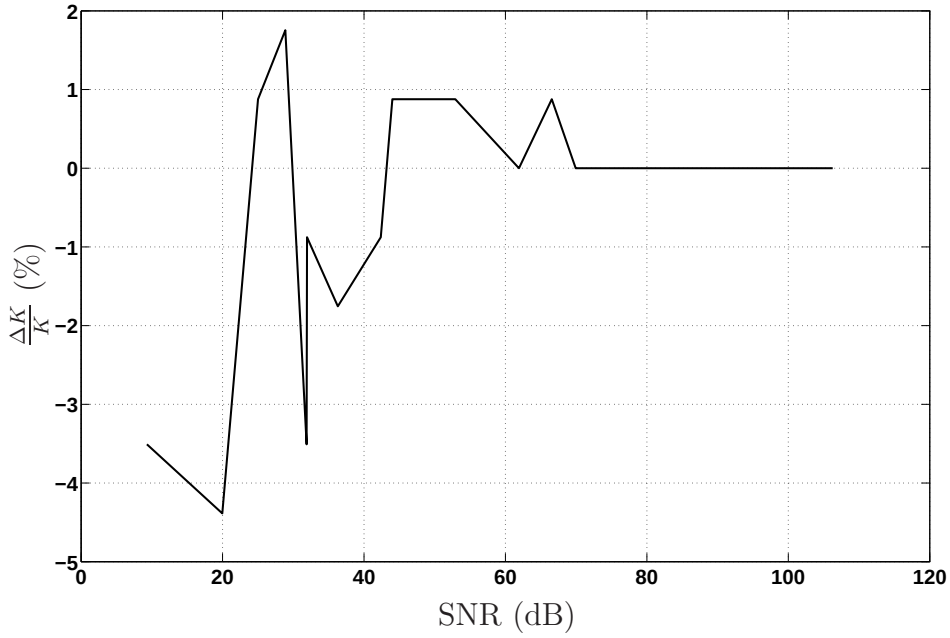

Figure 6: Enumeration accuracy as a function of the signal-to-noise ratio.

The results of the test are displayed in Figure 6. They show that the method is very accurate when the noise level is weak: the estimation error is quasi-null for SNR values larger than 70 dB. When the noise is no longer insignificant, the method accuracy deteriorates, yet still good, the estimation

error being less than 5 % for SNR values larger than 40 dB. In practice, the SNR is usually larger than 50 dB.

Influence of the driving-point

The driving-point may be influential on the method accuracy: the sinusoid amplitudes are controlled by the driving-point position. Sinusoids with a small amplitude are quickly drowned into noise, making them undetectable. For the test, every parameter is set to its nominal value, and solely the driving-point is modified. Positions follow a mesh spanning the bottom-left quadrant of the simulated plate (the results on the other quadrants are the same by symmetry). The results are displayed in Figure 7.

The effect of nodal lines is obvious: positions for which the normalised positions x/L_x and y/L_y are simple ratios (1/2, 2/5, 1/3, 1/4, and 1/5) lead to the largest errors of estimation. For these positions, numerous modes are excited at their node positions, hence a larger error of estimation. For other positions, the estimation is accurate (less than 2 %).

3.2. Tests on realistic simulated impulse response of flat panels

3.2.1. Presentation of the tests

The ability of the method to estimate the Young modulus and the mass density of 47 simulated plates is tested in this section. The dimensions of the plates are set to a unique arbitrary value for all of them : $L_x = 400$ mm, $L_y = 280$ mm, and $h = 2.5$ mm. Modal loss factors are the same for every mode and for every plate. The value is set to 1 %. The values of the Young modulus and the mass density are chosen so that they correspond to typical values of different kind of materials:

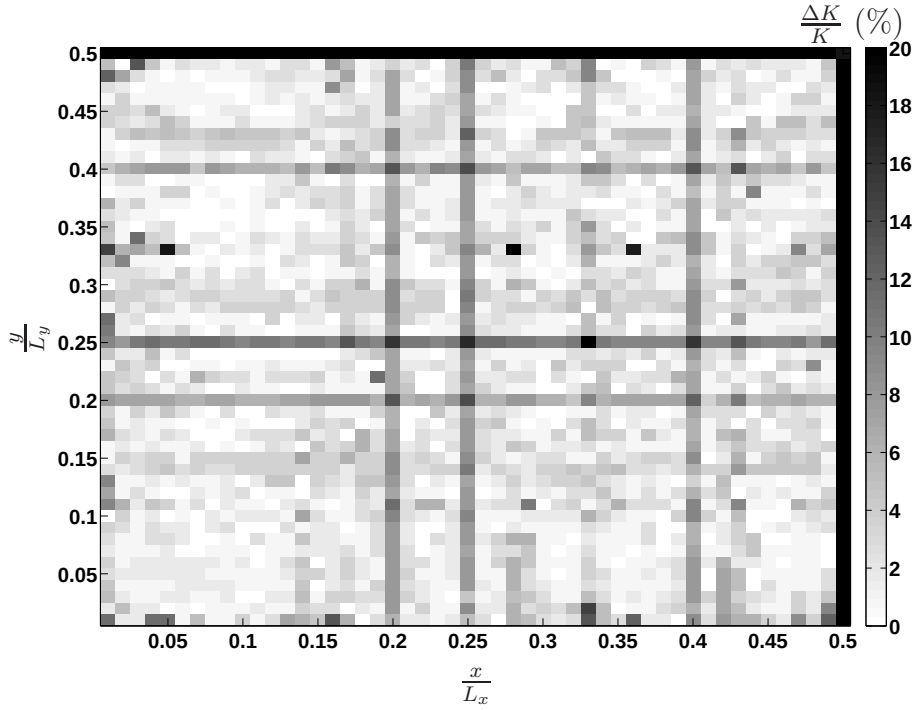

Figure 7: Error of estimation on the number of modes as a function of the driving-point position on the bottom-left quadrant of the simulated plate.

1. Softwood (Cedar, Pine, Spruce, ...)
2. Hardwood (Mahogany, Maple, Oak, ...)
3. Polymers (Poly(methyl methacrylate), Carbon fibers, ...)
4. Metals (Aluminum, Iron, Gold, ...)

The properties of the materials are displayed in Figure 8. In real life, softwood and hardwood are orthotropic materials, and present different Young moduli. For the tests, we chose a single equivalent Young modulus E^*, computed from Eq. (8).

The method is then applied an hundred times to each simulated plate. The driving-point position is randomly set, according to an uniform distribu-

tion within the plate dimensions, limited to the second and third quartiles of each dimension ($x \in \left[\frac{L_x}{4} \quad 3\frac{L_x}{4}\right]$ and $y \in \left[\frac{L_y}{4} \quad 3\frac{L_y}{4}\right]$). The analyzed signals are the mean signals of 5 simulated impulse responses, corresponding to 5 different driving-points.

3.2.2. Results

Results are displayed in Figure 8. The estimated values of E and ρ are systematically close to the theoretical values, with a negligible deviation. The estimation bias is within a range from 0 to 10 %.

The tests shows that the method enables a robust estimation of the mechanical parameters of the flat panels using a few driving-point transfer function measurements, 5 in this example, located at randomly chosen positions. The presented method enables a straightforward characterization of materials used by luthiers for musical instrument manufacturing. Besides, these macroparameters are discriminant. Indeed, materials of the same class group together in the Ashby diagram: their Young modulus and mass density have the same order of magnitude.

4. Experimental results

4.1. Experimental protocol

Two plates have been tested: one is a steel square plate, the other one is a red cedar plate, used for guitar soundboard manufacturing. Panels are hung with wires, fixed to their upper corners. This experimental setup is intended to approach free-edge boundary conditions, while minimizing the added dissipation due to suspensions. The impulse response $s(t)$ is obtained

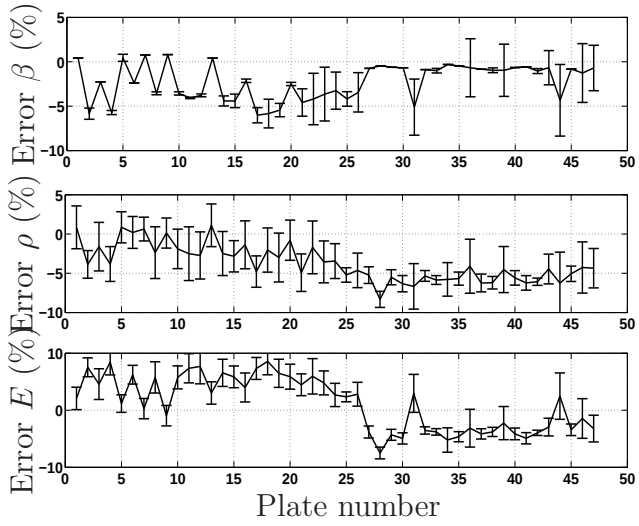

(a)

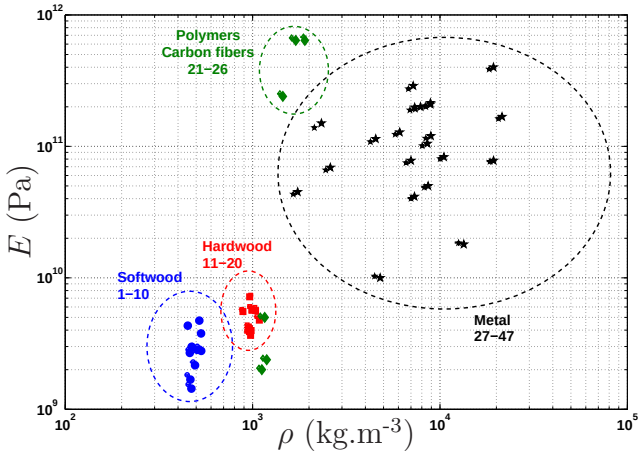

(b)

Figure 8: a) Median value of the errors of estimation of the macroparameters β, ρ, and E for the 47 plates. The error bars represent the median absolute deviation of each set of 100 simulations. b) Theoretical values (large symbols) and estimated values (small symbols) of E and ρ for the 47 plates.

Table 2: geometric and mechanical properties of the steel plate.

Parameter	Unit	Value
Plate length	m	0.24
Plate width	m	0.24
Plate thickness	m	4.6×10^{-3}
Young's modulus	GPa	200
mass density	$kg.m^{-3}$	7623
Plate mass	kg	2.02

by a synchronous and co-localized measurement of the excitation signal, using a small impact hammer (PCB Piezotronics 086E80), and the acceleration signal, by means of a small accelerometer (PCB Piezotronics 352C23, 0.2g). The plate is impacted at the same point than the measurement and the process is repeated thrice. The experimental protocol is displayed in Figure 9. The analyzed signal is the average of the impulse responses obtained from the three acquisitions. This is therefore a non-physical signal, yet it contains the physical eigenmodes of the system. The interest of the averaging is to avoid weak sinusoids due to nodal lines.

4.2. Results

4.2.1. Steel plate

The geometry and the mechanical properties of the steel plate are shown in Table 2. Since the steel is an alloy, its mechanical properties can vary. However, the typical values are in the same order of magnitude. A Young's modulus of 200 GPa is typical of steel alloys.

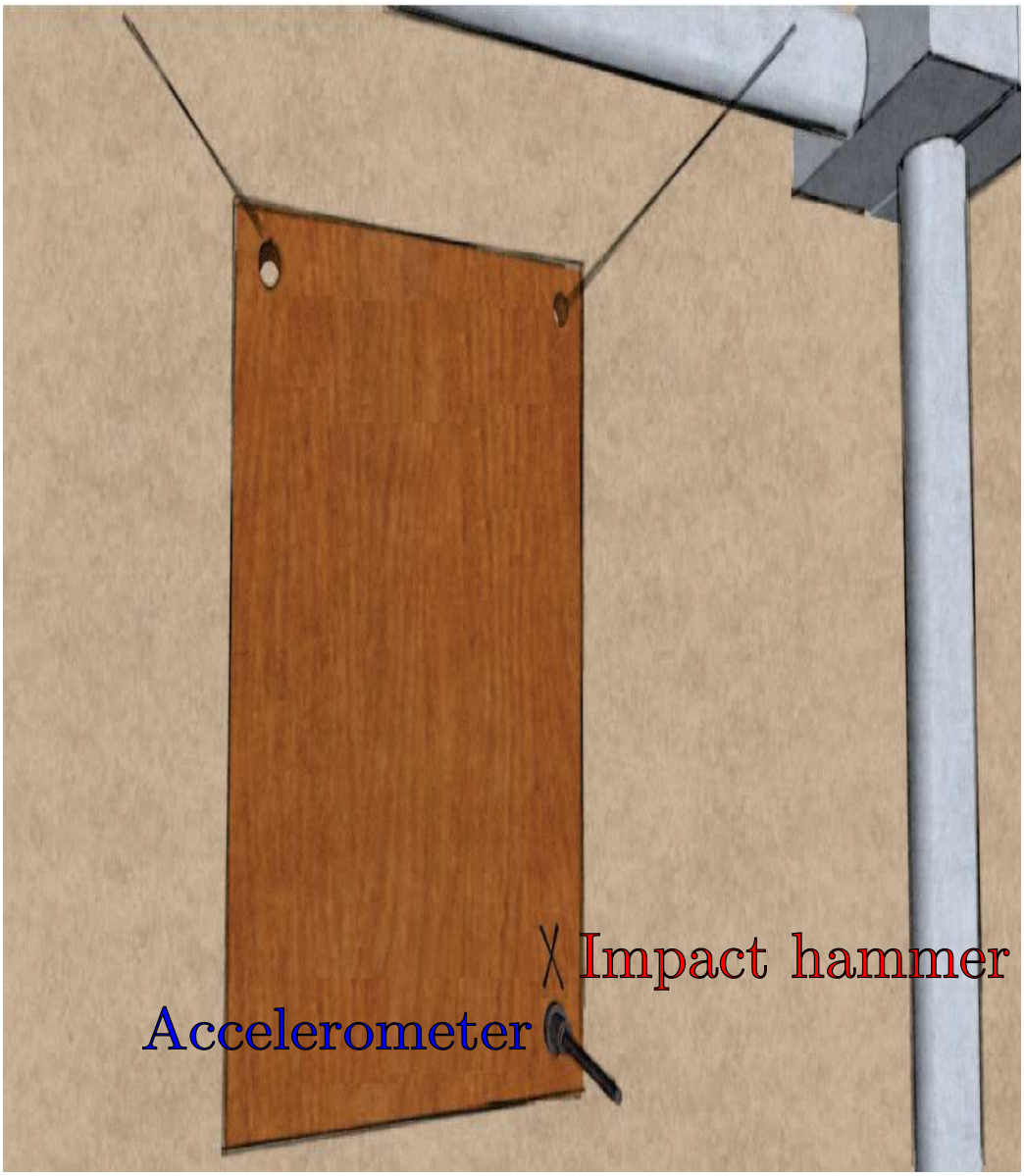

Figure 9: Experimental setup for panel mobility measurement.

Modal density

Figure 10 shows the modal density estimated via the modal frequencies given by ESPRIT. The mobility computed from the modal parameters

estimated by ESPRIT is in good agreement with the measured mobility, indicating that the modal parameter estimation is correct.

The modal density shows a typical behavior of a flat panel with free edges: it is slightly decreasing, tending toward a constant value in the high frequency range. this asymptotic value is around 0.0055 mode per Hz, which means one mode every 180 Hz. The comparison with the analytical modal density of the plate with typical properties of the steel confirms the good accuracy of the estimation, they are indeed very close, and are in good agreement with the discrete modal density computed from the modal frequencies estimated by ESPRIT.

Young's modulus and mass density

The direct weighing of the panel gives the mass density: 7623 kg.m^{-3} (*cf.* Table 2). The mass density estimated via the present method is close to the value obtained from direct weighing (0.08 %). The estimated Young's modulus is 192 GPa, the difference with the typical value is 8 GPa. This difference represents 9.6 %, showing that the results are in good agreement with expected values. It shows that the steel alloy, used to make this panel, is rather flexible ahead of typical steel alloys. The mass density is estimated with an error less than 0.1 %, and the estimated Young's modulus is in the order of magnitude of that of steel alloys.

Modal loss factor

Figure 11 shows the estimated loss factor of the steel plate as a function of the frequency. It shows very low value, which is typical of metallic materials.

The modal loss factor profile shows a sudden increase at frequencies higher

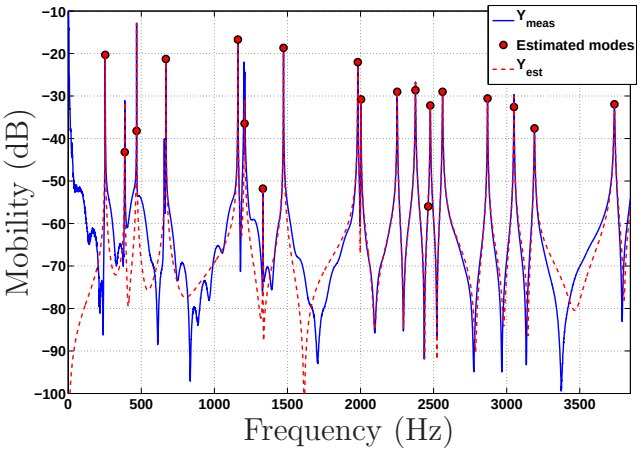

(a)

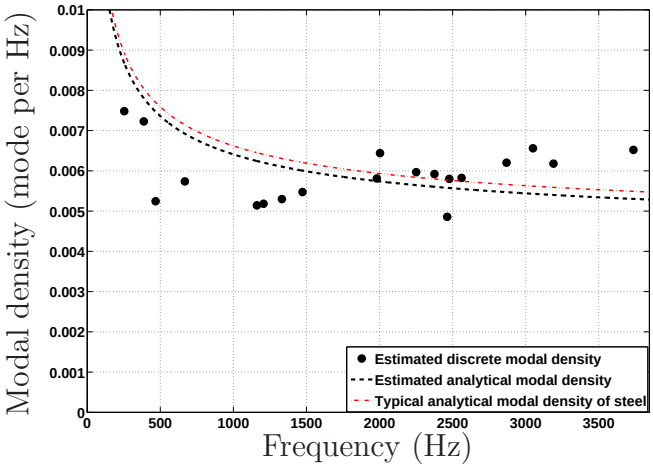

(b)

Figure 10: a) measured mobility and estimated mobility of the steel plate, computed from the modal parameters estimated by ESPRIT. The estimated mode positions are denoted by circles. b) Discrete modal density estimated by ESPRIT and estimated analytical modal density. The analytical modal density of the plate having typical mechanical properties of the steel (*cf.* Table 2) is plotted for comparison.

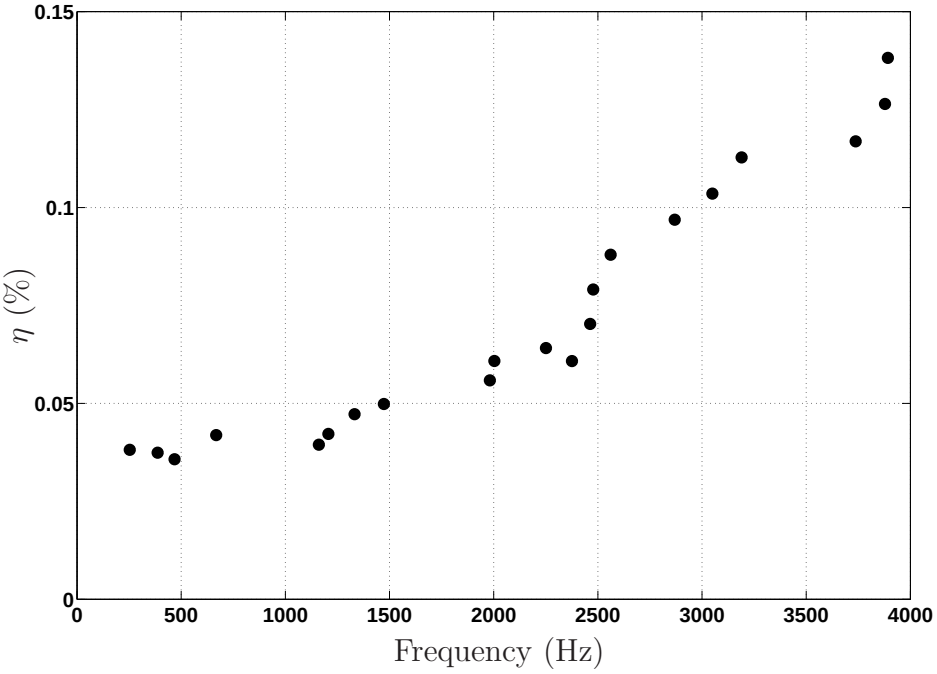

Figure 11: Estimated loss factor as a function of the frequency of the steel plate.

than 2200 Hz. This increase might be due to radiation losses. Indeed, for finite plates, the radiation is weak below a certain frequency, called *critical frequency*, and becomes important at higher frequencies [37]. The critical frequency depends on the mechanical properties of the plate and on the sound velocity c_a of the acoustic waves in the surrounding fluid:

$$f_c = \frac{c_a^2}{2\pi}\beta. \tag{21}$$

In the case of the studied steel plate in the air, the critical frequency, computed from Eq. (21), with $c_a = 343$ m.s^{-1}, is around 2550 Hz, which is in agreement with the observed increase of the loss factor in Figure 11.

Table 3: Properties of the red cedar plate. The bending stiffness values are those estimated by Růžek.

Parameter	Unit	Value
Plate length	m	0.5
Plate width	m	0.19
Plate thickness	m	2×10^{-3}
Mass density	kg.m^{-3}	427.5
Plate mass	kg	0.102
D_1	N.m	9.52
$D_2 + D_4$	N.m	4.89
D_3	N.m	0.94
D^*, after Eq. (7)	N.m	2.86

4.2.2. Red cedar plate

The method is now applied to a red cedar plate, used for guitar soundboard manufacturing. The geometry and the mechanical properties of the plate are shown in Table 3.

Modal density

As for Figure 10, Figure 12 shows the modal density estimated via the modal frequencies given by ESPRIT. The mobility computed from the modal parameters estimated by ESPRIT is in good agreement with the measured mobility, indicating that the modal parameter estimation is correct.

The discrete modal density estimated by ESPRIT is similar to typical modal density profile of freely vibrating plates: it slightly decreases with frequency and tends toward a constant value in the high frequency range. It

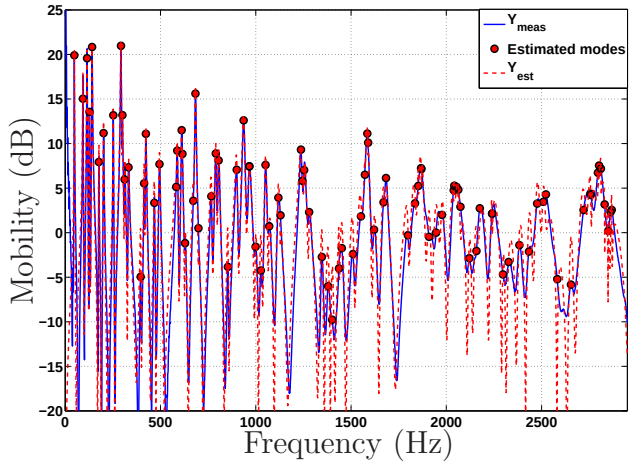

(a)

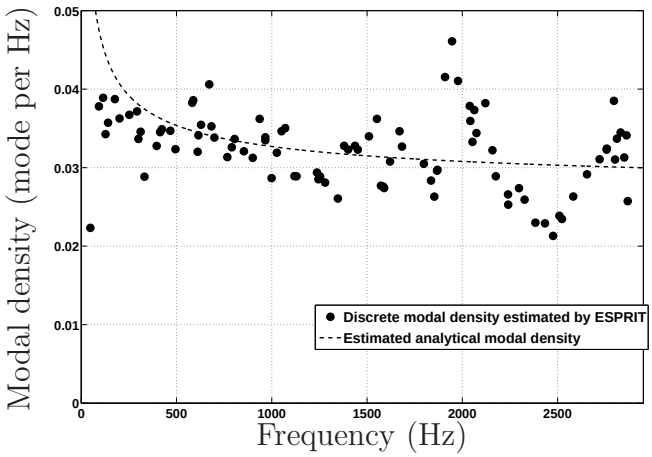

(b)

Figure 12: a) measured mobility and estimated mobility of the red cedar plate, computed from the modal parameters estimated by ESPRIT. The estimated mode positions are denoted by circles. b) Discrete modal density estimated by ESPRIT and estimated analytical modal density.

also exhibits a few local maxima and minima located around the analytical value of the modal density, since the wood plate is both bidimensional and orthotropic. Eigenmodes are in fact not evenly distributed, leading sometimes to very close or very distant consecutive modes, which results in local extrema in the discrete modal density.

Young's modulus and mass density

The estimated mass density is 411 kg.m^{-3}, which corresponds to a 4 % bias with the theoretical value, 427.5 kg.m^{-3}. The estimated bending stiffness is 2.84 N.m. This value can be compared with the bending stiffness estimated by M. Růžek, using a method derived from the RIFF method [38] and a method developed by Chardon *et al.* [39]. This method estimates the bending stiffness of the studied red cedar plate at 2.86 N.m, which is similar to the estimated bending stiffness, using our method (the difference is 0.79 %). This shows that the method presented in this paper gives results very similar to independent methods. Consequently, it is possible to estimate a bending stiffness of an orthotropic plate.

Modal loss factor

Figure 13 shows the estimated loss factor of the red cedar plate. It shows a constant value slightly larger than 1 %. This profile has been previously observed in studies on wood materials [1, 40, 41]. The expected critical frequency for this structure is above 10 kHz, which is beyond the frequency band of analysis: unlike for the steel plate, the modal loss factor of the red cedar plate does not exhibit a sudden increase in the analyzed frequency band. The radiation effect is then not observable.

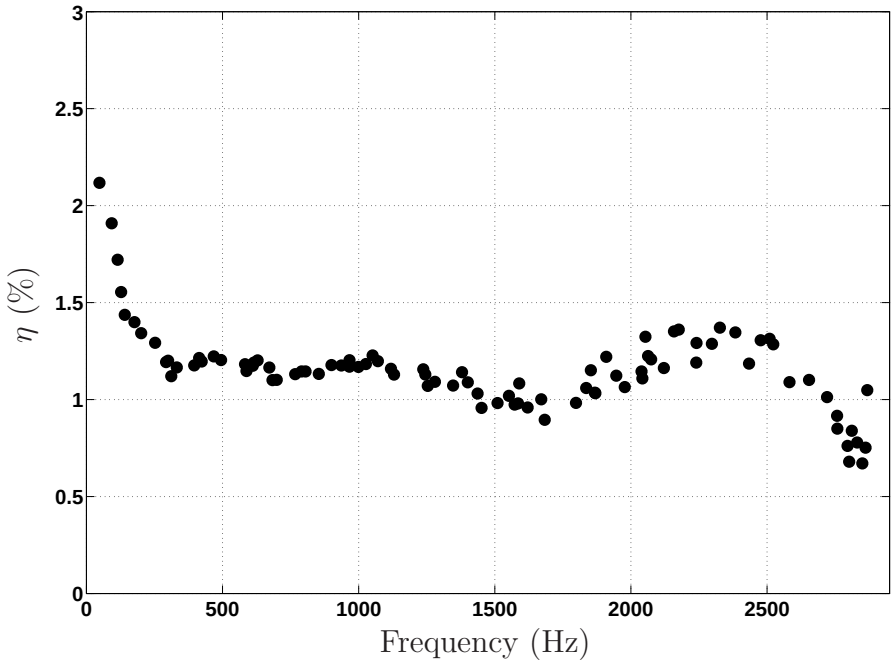

Figure 13: Estimated loss factor as a function of the frequency of the red cedar plate.

5. Conclusions

The study presented in this paper shows that it is possible to estimate, with good accuracy, the Young modulus and the mass density of flat panel, with solely a few measurement points, using affordable and easily handleable experimental devices. This method is therefore suitable for a daily practice in an artisan workshop, such as a luthier workshop for instance.

The method is based on an accurate estimation of the modal density of the structure and an estimation of the mean mobility. The modal density is estimated via the subspace method ESPRIT, associated with the signal enumeration technique ESTER. The mean mobility is computed as the mobility

of the equivalent structure with an infinite damping. The Young modulus and the mass density of the panel are estimated by fitting the experimental data with the theoretical expressions giving the modal density and the mean mobility.

The method is validated following different steps. First, the enumeration technique is tested using hybrid syntheses, aiming at reproducing experimental conditions. Simulations show that the enumeration is accurate as long as the modal overlap does not exceed 100 %, namely in the low and the mid-frequency domains. The second step tests the method for estimating the Young modulus and the mass density of a lot of 47 simulated plates. It shows that the Young modulus and the mass density can be estimated, with an error systematically less than 10 %, with 5 driving-point transfer function measurements, located at random positions.

Experimental applications of the method on metallic and wood plates confirm its ability to accurately estimate the characteristic parameters of the flat panel with a few driving-point transfer function measurements. For these applications, solely 3 measurements were performed. The mass density of a metallic plate is estimated, according to an error less than 0.1 % and less than 4 % for a wood plate.

The method can be applied in the instrument making context and will be implemented in the lutherie assistance system PAFI (*Plateforme d'aide à la facture instrumentale*).

Acknowledgements

The authors would like to acknowledge the *Agence Nationale pour la Recherche* for the financial support of the PAFI project (*Plateforme d'Aide à la Facture Instrumentale*).

References

[1] S. Yoshikawa, Acoustical classification of woods for string instruments, J. Acoust. Soc. Am. 122(1) (2007) 568–573.

[2] I. Brémaud, Acoustical properties of wood in string instruments soundboards and tuned idiophones: Biological and cultural diversity, J. Acoust. Soc. Am. 131(1) (2012) 807–818.

[3] M. Ashby, Y. Bréchet, D. Cebon, L. Salvo, Selection strategies for materials and processes, Materials and Design 25(1) (2004) 51 – 67.

[4] L. Garibaldi, M. Sidahmed, Matériaux viscoélastiques: Atténuation du bruit et des vibrations, Techniques de l'ingénieur N1 (N720) (2007) 1776–0178.

[5] K. P. Menard, Dynamic Mechanical Analsis : A practical introduction, Second edition, CRC Press, 2008.

[6] H. Oberst, K. Frankenfeld, Uder die dampfungder biegeschwingungen dunner bleche durch festhaftende belage, Acustica 2 (1952) 181–194.

[7] H. Niemann, J. Morlier, A. Shahdin, Y. Gourinat, Damage localization using experimental modal parameters and topology optimization, Mechanical Systems and Signal Processing 24 (3) (2010) 636 – 652.

[8] H. Koruk, K. Y. Sanliturk, Identification and removal of adverse effects of non-contact electromagnetic excitation in oberst beam test method, Mechanical Systems and Signal Processing 30 (0) (2012) 274 – 295.

[9] A. Birks, R. E. J. Green, P. M. Intyre, Nondestructive testing handbook, Vol. 7, 2nd edition, American Society for nondestructive testing, 1991.

[10] J. Jiao, W. Liu, J. Zhang, Q. Zhang, C. He, B. Wu, Time-frequency analysis for ultrasonic measurement of liquid-layer thickness, Mechanical Systems and Signal Processing 35 (1-2) (2013) 69 – 83.

[11] D. Cernadas, C. Trillo, Ángel F. Doval, Óscar López, C. López, M. P.-A. Benito V. Dorrío, José L. Fernández, Non-destructive testing of plates based on the visualisation of lamb waves by double-pulsed tv holography, Mechanical Systems and Signal Processing 20 (6) (2006) 1338 – 1349.

[12] M. Géradin, D. Rixen, Théorie des vibrations. Application à la dynamique des structures, Ed. Masson Paris, 1992.

[13] T. K. Caughey, Classical normal modes in damped linear dynamic systems, J. Appl. Mech. 27(2) (1960) 269–271.

[14] D. J. Ewins, Modal Testing, Research Studies Press, 1984.

[15] N. M. M. Maia, J. M. M. Silva, Modal analysis identification techniques, Phil. Trans. R. Soc. Lond. 359 (2001) 29–40.

[16] R. H. Lyon, Statistical Energy Analysis of Dynamical Systems: Theory and Applications, MIT Press, Cambridge, 1975.

[17] J. Berthaut, M. N. Ichchou, L. Jézéquel, Piano soundboard: Structural behavior and numerical and experimental study in the modal range, Applied Acoustics 64 (2003) 1113–1136.

[18] R. O. Smith, Multiple emitter location and signal parameter estimation, in: Proc. RADC Spectrum Estimation Workshop, 1979, pp. 243–258.

[19] Y. Hua, T. K. Sarkar, Matrix pencil method for estimating parameters of exponentially damped/undamped sinusoids in noise, IEEE Trans. Acoust. Speech Sig. Process. 38(5) (1990) 814–824.

[20] R. Roy, T. Kailath, Esprit – estimation of signal parameters via rotational invariance techniques, IEEE Transactions on Acoustics Speech and Signal Processing 37(7) (1989) 984–995.

[21] J.-L. Le Carrou, F. Gautier, R. Badeau, Sympathetic string modes in the concert harp, Acta Acustica united with Acustica 95(4) (4) (2009) 744–752.

[22] B. David, Caractérisations acoustiques de structures vibrantes par mise en atmosphère raréfiée, Ph.D. thesis, Université Pierre and Marie Curie - Paris VI (1999).

[23] R. Badeau, B. David, G. Richard, A new pertubation analysis for signal enumeration in rotational invariance techniques, IEEE Transactions on Signal Proceeding 54(2) (2006) 450–458.

[24] K. Ege, D. Boutillon, B. David, High-resolution modal analysis, J. of Sound and Vibration 325 (2009) 852–869.

[25] J. Laroche, The use of the matrix pencil method for the spectrum analysis of musical signals, J. Acoust. Soc. Am. 94(4) (1993) 1958–1965.

[26] B. Elie, F. Gautier, B. David, Macro parameters describing the mechanical behavior of classical guitars, J. Acoust. Soc. Am. 132(6) (2012) 4013–4024.

[27] I. Santamaria, C. Pantaleon, J. Ibaez, A comparative study of high-accuracy frequency estimation methods, Mechanical Systems and Signal Processing 14(5) (2000) 819 – 834.

[28] G. Bienvenu, L. Kopp, Optimality of high-resolution array processing using the eigensystem method, IEEE Trans. Acoust. Speech Sig. Process. 31(5) (1983) 1235–1245.

[29] M. Wax, T. Kailath, Detection of signals by information theoretic criteria, IEEE Trans. Acoust. Speech Sig. Process. 33(2) (1985) 387–392.

[30] H. Akaike, Information theory and an extension of the maximum likelihood principle, in: Proc. of the 2nd International Symposium on Information Theory, 1973.

[31] G. Schwarz, Estimating the dimensions of a model, The Annals of Statistics 6(2) (1978) 461–464.

[32] R. Courant, D. Hilbert, Methods of Mathematicals Physics and Vol. 1, Wiley Classic edition, 1989.

[33] J. P. D. Wilkinson, Modal densities of certain shallow structural elements, J. Acoust. Soc. Am. 43(2) (1968) 245–251.

[34] G. Xie, D. J. Thompson, C. J. C. Jones, Mode count and modal density of structural systems : Relationships with boundary conditions, J. of Sound and Vibration 274(3) (2004) 621–651.

[35] E. Skudrzyk, The mean value method of predicting the dynamic response of complex vibrators, J. Acoust. Soc. Am. 67(4) (1980) 1105–1135.

[36] I. Elishakoff, Distribution of natural frequencies in certain structural elements, J. Acoust. Soc. Am. 57(2) (1975) 361–369.

[37] G. Maidanik, Response of ribbed panels to reverberant acoustic fields, J. Acoust. Soc. Am. 34(6) (1962) 809–826.

[38] C. Pezerat, Q. Leclere, N. Totaro, M. Pachebat, Identification of vibration excitations from acoustic measurements using near field acoustic holography and the force analysis techniques, J. of Sound and Vibration 326 (2009) 540–556.

[39] G. Chardon, A. Leblanc, L. Daudet, Plate impulse response spatial interpolation with sub-Nyquist sampling, J. of Sound and Vibration 23(7) (2011) 5678–5689.

[40] M. E. McIntyre, J. Woodhouse, On measuring the elastic and damping constants of orthotropic sheet materials, Acta Metallurgica 36(6) (1988) 1397–1416.

[41] T. Ono, S. Miyakoshi, U. Watanabe, Acoustic characteristics of unidirectionally fiber-reinforced polyurethane foam composites for musical

instrument soundboards, Acoustical Science and Technology 23(3) (3) (2002) 135–142.